NASA SP-330

APOLLO 17

Preliminary Science Report

PREPARED BY

LYNDON B. JOHNSON SPACE CENTER

Scientific and Technical Information Office 1973

NATIONAL AERONAUTICS AND SPACE ADMINISTRATION

Washington, D.C.

23. Ultraviolet Spectrometer Experiment

William G. Fastie,[a†] *Paul D. Feldman,*[a] *Richard C. Henry,*[a] *H. Warren Moos,*[a] *Charles A. Barth,*[b] *Gary E. Thomas,*[b] *Charles F. Lillie,*[b] *and Thomas M. Donahue*[c]

An ultraviolet spectrometer (UVS) on board the Apollo 17 orbiting spacecraft was used in an attempt to measure ultraviolet emissions from the lunar atmosphere. The only emissions observed in the lunar atmosphere were from a transient atmosphere introduced by the lunar module descent engine; 4 hr after the lunar module landed, these emissions were no longer detectable by the spectrometer. The absence of atomic hydrogen (H) expected to be present from the solar wind source leads to the conclusion that solar wind protons are neutralized and converted to molecular hydrogen (H_2) at the lunar surface.

During crossings of the solar-illuminated surface, the spectrometer measured significant variations in surface albedo. These variations are ascribed to variations in the refractive index of the lunar surface material.

The spectrometer made a number of nonlunar observations in lunar orbit and during transearth coast (TEC), including a search for the ultraviolet zodiacal light, solar atmosphere emissions, Earth emissions (including those from the geomagnetic tail), stellar emissions, and galactic emissions. Although significant data were obtained from all these observations, analysis of the data requires precise spacecraft attitude information in galactic coordinates; this information has not yet been received. During TEC, the fluorescence spectrum of H_2 was observed during a purge of the Apollo 17 fuel cells.

INSTRUMENT DESCRIPTION AND CALIBRATION

The Apollo 17 UVS has been described in great detail elsewhere (ref. 23-1). In summary, it is of the Ebert type, which has been broadly used for space research, but employed new optical and electronic techniques that provided about an order of magnitude improvement in sensitivity. These improvements included exit slit mirrors that provided a 2.5 increase in the signal to the detector pulse-counting electronics (which permitted detection of single photoelectrons) and a precision wavelength scan system that permitted the summation of a large number of spectra without loss of spectral resolution.

The spectrometer is shown in figure 23-1. The triangular stand on which the instrument was mounted (fig. 23-1(a)) was attached to a spacecraft bulkhead that was perpendicular to the spacecraft longitudinal axis. The large baffle over the entrance slit excluded stray light and was designed with multiple angles in several sections to provide a very large capability for rejection of unwanted radiation. There were no external optical components.

As seen in figure 23-1(b), light rays passing through the spectrometer entrance slit are rendered parallel by an area on one side of the spherical Ebert mirror, which directs the rays to the grating. Diffracted rays from the grating go to the area on the other side of the Ebert mirror that focuses the rays through the entrance slit to the face of a solar-blind photomultiplier tube, which transforms each photoelectron produced by a photon into several million electrons. An accumulator circuit counts and stores these pulses for 0.1 sec, and the accumulated pulse count is transmitted to the spacecraft data system as a 16-bit word.

The wavelength scan system consisted of a synchronous, motor-driven, cyclical cam, which encapsulated the pin on a follower arm. The follower arm was attached to the grating shaft. The 3600-lines/mm grating was rotated approximately 5° by the cam drive system to scan the spectral region 118 to 168

[a]The Johns Hopkins University.
[b]University of Colorado.
[c]University of Pittsburgh.
[†]Principal Investigator.

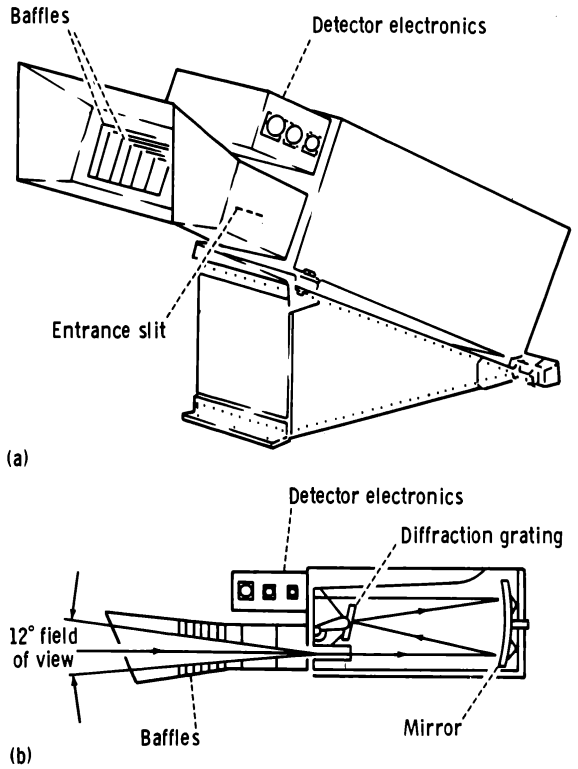

FIGURE 23-1.–Ultraviolet spectrometer. (a) Isometric view of the instrument mounted on a stand, which was attached to a bulkhead in the scientific instrument module bay of the Apollo 17 spacecraft. (b) Optical ray diagram.

nm once every 12 sec. The cam was programed to scan linearly in wavelength at the rate of approximately 7.5 nm/sec except for two 5-nm regions centered at 121.6 and 147.0 nm, where the scan rate was approximately 1.7 nm/sec to give temporal preference to Lyman-alpha radiation (121.6 nm) and to the resonance line of the heaviest atmospheric gas xenon (Xe) at 147.0 nm. The 144.5- to 149.5-nm region also included a fluorescent line of molecular hydrogen and one of carbon monoxide (CO).

The sensitivity S of the spectrometer to a gas column that is emitting 1×10^6 photons/sec-cm^2 (1 R) is given by

$$S\ (\text{counts/sec}) = \frac{1 \times 10^6}{4\pi} \frac{A_s A_g}{F^2} QT \qquad (23\text{-}1)$$

where A_s = slit area $\approx$ cm^2 (1-nm resolution)
A_g = grating area $\approx 1 \times 10^2$ cm^2
F = spectrometer focal length = 50 cm
Q = quantum efficiency of the detector ≈ 10 percent
T = transmission of the optical system ≈ 30 percent

or

$$S\ (\text{counts/sec}) \approx 100\ \text{photoelectrons/sec/R} \qquad (23\text{-}2)$$

To provide precision measurements with the spectrometer, it is necessary to measure the value of Q over the exposed area of the photomultiplier tube and to measure the transmission of the optical system over the entire field of view of the spectrometer. No standard source exists for the far ultraviolet region, and a spatially uniform reference source to fill the wide aperture of the spectrometer is beyond the state of the art. A high-precision calibration was accomplished in a specially built vacuum facility, which provided an intense, high f-number, monochromatic beam that could be focused into a very small spot on any point of the entrance slit. The flight spectrometer was mounted in the vacuum chamber on a tilting platform so that the calibrating beam could be directed through the entrance slit to each area of the diffraction grating. A calibrated photomultiplier tube could be inserted in the monochromatic beam to measure the number of photons passing through the entrance slit. A National Bureau of Standards calibrated photodiode was used to calibrate the reference photomultiplier tube before and after each calibration of the spectrometer.

The calibration was performed at a total of 10 wavelengths in the spectral region that the instrument scanned. Successive calibrations provided very reproducible sensitivity values at all wavelengths. A cross-check of the system was provided by calibration of a spare instrument in the vacuum optical bench at the NASA Goddard Space Flight Center, which confirmed the absolute value of the calibration. We believe these careful techniques ensure that the signals observed in flight were measured to an accuracy of ± 10 percent.

LUNAR ATMOSPHERE OBSERVATIONS

The Apollo 17 UVS experiment has as its primary objective the measurement of the density and composition of the lunar atmosphere by observing resonance scattering and fluorescence of solar far ultra-

violet radiation. This technique can provide density measurements in the range 1×10^1 to 1×10^4 atoms/cm^3 for H, H_2, atomic oxygen (O), carbon (C), atomic nitrogen (N), CO, carbon dioxide, and Xe but, because of spectral range limitations, could not measure helium, neon, or argon-36, all of which may be present as major constituents of the lunar atmosphere, if the solar wind is the major source for the atmosphere. In addition, radiogenic argon-40 (^{40}Ar) from potassium-40 decay should be present. The present results indicate that the surface concentration of atomic hydrogen is less than 10 atoms/cm^3, almost three orders of magnitude less than predicted (ref. 23-2), whereas the concentration of H_2, if present, is less than 6.0×10^3 atoms/cm^3. This is consistent with the hypothesis that the solar wind protons are completely converted into hydrogen molecules at the lunar surface. None of the other observable constituents were detected. A transient atmosphere was observed shortly after lunar module touchdown but disappeared in a matter of hours. No evidence of outgassing was detected in the vicinity of the crater Aristarchus, where many transient optical phenomena have been reported.

Previous measurements of the lunar atmosphere based on an in situ pressure gage (ref. 23-3) indicated that the total surface density at the subsolar point may be as small as 1×10^7 atoms/cm^3. More recently, mass spectrometer measurements from lunar orbit (ref. 23-4) and from the lunar surface (ref. 23-5) have resulted in detection of neon, argon, and helium. Lunar outgassing, the only possible source of a substantial atmosphere, occurs at a rate several orders of magnitude less than the corresponding rate on Earth (ref. 23-6). Apart from ^{40}Ar and radiogenic helium (ref. 23-7), the lunar atmosphere may consist only of neutralized solar wind ions. Thus, the lunar atmosphere would be expected to be composed primarily of neon, argon, hydrogen, and helium, the subsolar surface concentrations of which would lie in the range 2×10^3 to 7×10^3 atoms/cm^3 (ref. 23-7).

The Apollo 17 UVS was mounted in the scientific instrument module (SIM) with the optic axis pointed 23° forward and 18° right of the SIM center line (when looking toward the spacecraft nose). The SIM center line nominally pointed through the center of the Moon when the spacecraft was constrained to local horizontal attitude. Atmospheric observations were made in various spacecraft attitudes as shown in figure 23-2. The principal mode of operation was the

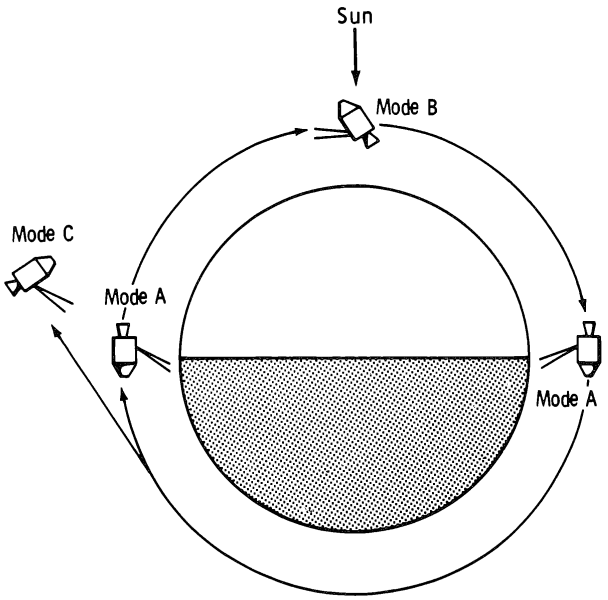

FIGURE 23-2.–Schematic representation of the modes of observation of the lunar atmosphere. Mode A, the principal orbital mode, consists of observation through the illuminated atmosphere above the terminator against the dark side of the Moon. In mode B, a contingency orbital mode, the spectrometer is pointed at a fixed point in space, and the line of sight extends through a tangential slice of illuminated atmosphere. Mode C was used immediately after transearth injection. The Apollo 17 UVS has a field of view of 12° by 12° and looks forward 23° relative to the normal to the spacecraft longitudinal axis.

observation through the illuminated atmosphere above the terminator against the dark side of the Moon (mode A in fig. 23-2). This was done automatically once per revolution if the spacecraft was maintained in the local horizontal attitude (twice if the spacecraft axis reversal was performed between terminator crossings). A total of 1200 of these terminator spectra was obtained.

To allow for the possibility that the atmospheric emissions might be too weak for detection in the principal mode, two special modes were provided to enhance the sensitivity. These modes resulted in most of the upper limits quoted herein. In the first mode, the spectrometer was pointed at a fixed point in space and, as the spacecraft moved in its orbit, the line of sight extended through a tangential slice of illuminated atmosphere (mode B in fig. 23-2). The enhancement provided by this mode is ≈ 20 for H and H_2 and ≈ 10 for O, based on Chamberlain's model of an evaporating corona with the lunar

surface as the critical level (ref. 23-8). The second mode (mode C in fig. 23-2) was used immediately after transearth injection (TEI) and is similar to mode A except for the much greater optical path length.

For all atmospheric constituents other than hydrogen (Lyman alpha, 121.6 nm), the sensitivity limit was set by the background count rate (≈ 25 counts/sec), which was caused by solar cosmic ray protons. At 121.6 nm, solar radiation resonantly scattered from hydrogen atoms in the interplanetary medium produces a background of between 200 and 400 R (depending on the viewing direction), in good agreement with previous measurements (ref. 23-9). Emission rates of 6 to 12 R (450 to 900 counts/sec) are obtained when the scattered radiation is observed after reflection from the surface of the dark side of the Moon. Solar Lyman alpha scattered from the Earth hydrogen geocorona and then reflected from the Moon beyond the lunar terminator adds a 1-R contribution to the background for crossings of the terminator facing Earth. During TEC, the fixed areas of space observed in the tangential mode (mode B in fig. 23-2) were again observed to provide a sky background correction for the tangential mode.

We define

$$N_i(z_1, z_2) = \int_{z_1}^{z_2} n_i(z')\,dz' \qquad (23\text{-}3)$$

where z_1 and z_2 are two altitudes above the lunar surface, and $n_i(z')$ is the density in atoms per cubic centimeter of atomic species i at altitude z', so that $N_i(0, z)$ is the vertical column density of that atomic species between the surface and altitude z. For observations at an angle θ to the local vertical, the emission rate $4\pi I_i$, in rayleighs, for resonance scattering of solar flux in the ith line is given by

$$4\pi I_i = 1 \times 10^{-6} g_i [N(0,z)][CH(\theta)] \qquad (23\text{-}4)$$

where g_i is the resonance g-factor and $CH(\theta)$ is the Chapman function (ref. 23-10). For molecular species, it is necessary to specify $g_{\nu',\nu''}$, where ν' and ν'' are vibrational quantum numbers of the excited and ground states, respectively. Table 23-I lists the transitions of interest, the resonance g-factors, the instrument sensitivity, and the minimum detectable concentration for the particular mode of observation.

Figure 23-3 shows the difference between the average of the sum of 70 spectra observed in mode B in lunar orbit and the average of 210 spectra obtained during TEC (mode C) when the spectrometer axis was pointed at the same point in space. The spacecraft altitude varied from 70 to 46 km, and the spacecraft was near the subsolar point throughout the observation. Wavelengths corresponding to the resonance transitions of O, C, Xe, and N, to the Lyman bands of H_2, and to the fourth-positive bands of CO are indicated. No emission features are apparent in the spectrum. Figure 23-4(a) shows a sum of 25 spectra

TABLE 23-I.—*Ultraviolet Spectrometer Observations*

Species	*Energy-state transition*	*Wavelength, nm*	*Resonance g-factor, photon/sec/molecule*	*Mode of observation*[a]	*Sensitivity, photoelectrons/sec/R*	*Observed surface density,*[b] *atoms/cm*^{3}
			Atomic			
H	$2S - 2P$	[c]121.6	2.2×10^{-3}	C	75	< 10
O	$3P - 3S$	130.4	2×10^{-5}	B	99	< 40
N	$4S - 4P$	120.0	3.6×10^{-6}	B	70	< 300
C	$3P - 3Po$	165.7	2.1×10^{-4}	B	25	< 15
Kr	$1S - 3P$	123.6	1.6×10^{-7}	A	85	< 10 000
Xe	$1S - 3P$	147.0	1.5×10^{-6}	A	75	< 1 000
			Molecular			
H_2	$B^1\Sigma_u^+ - X^2\Sigma_g^+$ (6, 9)	146.2	4.0×10^{-8}	B	75	< 6 000
CO	$A^1\Pi - X^1\Sigma^+$ (1, 0)	151.0	7.5×10^{-8}	B	60	< 20 000

[a]See figure 23-2.

[b]At the subsolar point, except for H, krypton (Kr), and Xe, which are terminator values. The entries in this column are based on the spectral feature not exceeding 1 standard deviation in the counting rate.

[c]Lyman alpha.

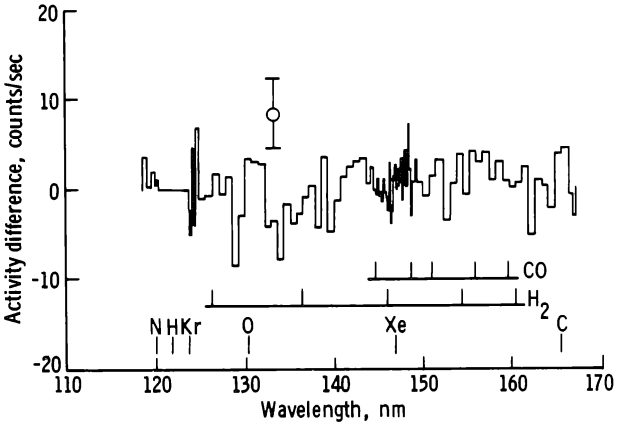

FIGURE 23-3.–The average of 70 spectra obtained during a tangential mode (mode B in fig. 23-2) observation with the sky background (observed during TEC) subtracted. The wavelengths of the principal emission features expected are indicated. The error bar represents 1 standard deviation in the observed counting rate.

obtained at the near-side terminator 2 hr after the lunar module had landed and indicates a slight enhancement at 130.4 nm (atomic oxygen) and at least one band of the CO fourth-positive system. None of these enhancements appear in figure 23-4(b), which shows the sum of 25 spectra obtained on the following orbit, 4 hr after landing.

In figure 23-5, the Lyman-alpha signal (121.6 nm) observed below the spacecraft between the terminator and a point 15° beyond the terminator (270° to 255°) (fig. 23-5(a)) is compared to the signal observed when the spacecraft was in full shadow (255° to 240°) (fig. 23-5(b)). The signal in figure 23-5(b) originated from solar radiation that was resonantly scattered from the solar system hydrogen atmosphere. The difference between the signals shown in figures 23-5(a) and 23-5(b) was initially misinterpreted as being of lunar atmospheric origin (ref. 23-1). More detailed data analysis, particularly of data from mode C (fig. 23-2), shows no signal that can be ascribed to an atomic hydrogen atmosphere to a limit of 10 atoms/cm^3 at the lunar surface. In mode C, the spacecraft altitude was increased by a factor of 5 with no increase in the Lyman-alpha (121.6 nm) signal. The signal difference (figs. 23-5(a) and 23-5(b)) is ascribed to an asymmetry in Lyman-alpha emission in the solar atmosphere. The existence of the asymmetry was confirmed by observations during TEC.

A number of conclusions emerge from the preceding results. The fact that xenon must be at best a minor component of the lunar atmosphere, despite its large mass (131.3), indicates that the mechanism of photoionization loss followed by acceleration in the solar wind electric field dominates over Jean's evaporative escape, at least for the heavy gases. The small concentrations of H, C, N, O, and CO, which are photodissociation products of many gases of volcanic origin, also place severe restrictions on present levels of lunar volcanism.[1] The most surprising result is the absence of atomic hydrogen to an upper limit almost three orders of magnitude below the predicted value (ref. 23-2). The effect of the terrestrial magnetic field in shielding the lunar surface from the incident solar wind proton flux would be important only late in the mission.[2] Other possible ways of accounting for the absence of hydrogen atoms are as follows.

1. Adsorption of solar wind protons in the lunar soil
2. Direct reflection of solar wind protons from the lunar surface
3. Neutralization and rapid escape from the lunar surface as suprathermal hydrogen atoms
4. Recombination to form molecular hydrogen

In current models of the interaction of the solar wind with the lunar soil (ref. 23-13), protons of $\approx$ 1-keV energy penetrate to a depth of $\approx 1 \times 10^{-6}$ cm. They will neutralize to form hydrogen atoms and may combine with other H atoms to form hydrogen molecules. Diffusion to the surface or into the dust grains to a depth of $\approx 1 \times 10^{-5}$ cm may occur. For adsorption within the soil to occur, the diffusion must be retarded, either by the formation of stable hydrides or by trapping in a lattice site. In either case, after sufficient exposure, the soil becomes saturated and diffusion from the surface will occur. Saturation occurs only for the outer surfaces of soil grains, which are exposed to the solar wind for periods ranging from 0.1×10^6 to 20×10^6 yr (ref. 23-14).

[1] The limits on the outgassing rates are being described in detail by G. E. Thomas et al.

[2] According to the empirical geomagnetic-tail model of Fairfield (ref. 23-11), the Moon should have entered the Earth bow shock 13 hr before the TEI maneuver. However, according to measurements of the solar wind at the surface of the Moon (ref. 23-12), the proton flux is not appreciably disturbed until the Moon enters the geomagnetic tail. The cut-off of solar wind flux should have occurred at approximately 18:00 G.m.t. on December 18, which was 44 hr after TEI.

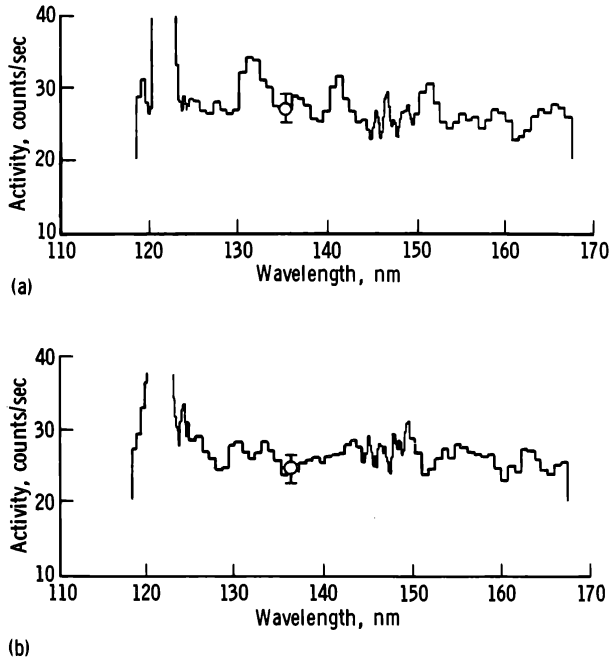

FIGURE 23-4.–Comparison of UVS spectra. The error bars represent 1 standard deviation in the observed counting rate. (a) Spectrum obtained 2 hr after lunar module landing, showing mild indication of emission features at 130.4 nm (O) and 151 nm (CO). (b) Spectrum obtained 4 hr after lunar module landing, showing no emission features.

Even for an exposure period of 1 million years (during which the solar wind is assumed constant), complete adsorption of the solar protons would give a density of 4 mg/cm^2 of hydrogen over the entire lunar surface. This value exceeds the measured composition of lunar soil by a factor of $\approx 1 \times 10^5$ (ref. 23-13).

The reflection of solar wind particles has been measured by several solar wind composition experiments on the lunar surface. The albedo for alpha particles is 10 percent (ref. 23-15), and the albedo for protons should not be significantly higher. In addition, significant reflection of solar wind ions would produce measurable perturbations of the solar wind magnetic field that have not been observed from lunar orbit (ref. 23-16).

A "sputtering" atmosphere of atomic hydrogen has been advocated (ref. 23-17), in which hydrogen atoms with average velocities of 15 km/sec are ejected from the lunar surface as a result of energetic ion impact. However, because hydrogen is a minor constituent of the lunar surface, the dominant com-

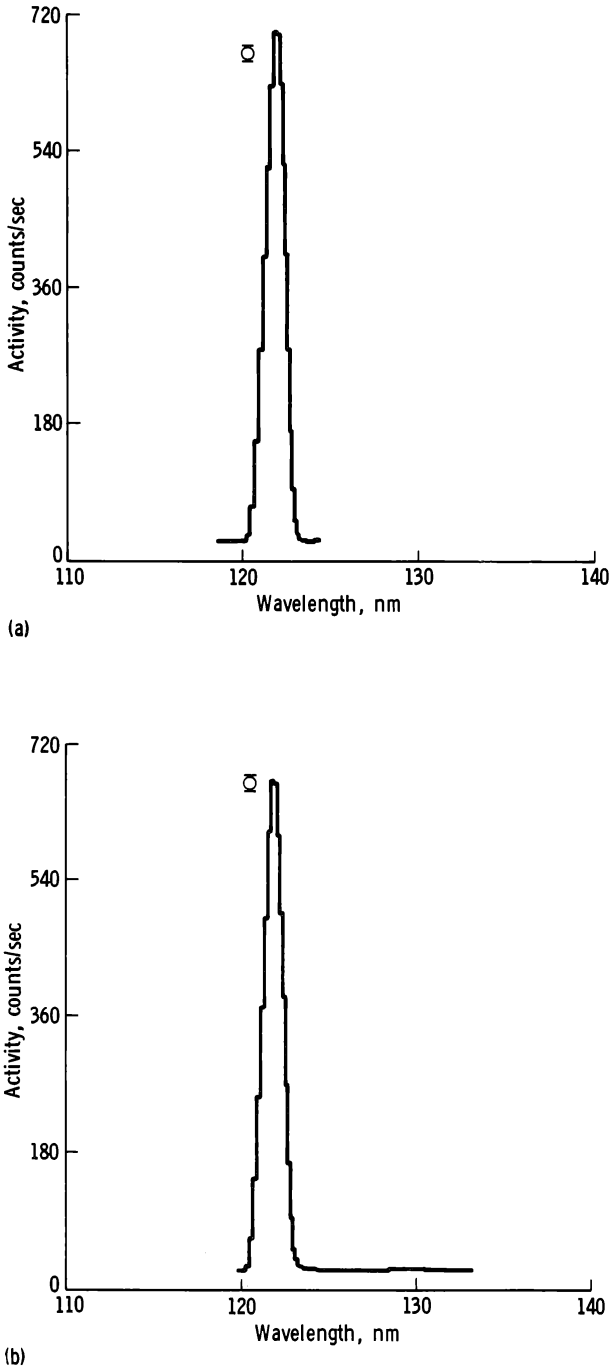

FIGURE 23-5.–Comparison of Lyman-alpha signals obtained on revolution 38. The signals are caused by reflected solar atmosphere radiation; the difference between the signals is due to asymmetry in the reflected solar radiation, not to a lunar H atmosphere. The error bars represent 1 standard deviation in the observed counting rate. (a) Signal observed just beyond the near-side terminator; coverage extends from 270° to 255°. (b) Signal observed when spacecraft was in full shadow; coverage extends from 255° to 240°

position of the sputtered material would probably be that of the lunar soil itself. Even if all the sputtered atoms were hydrogen with the previously mentioned average velocity, the maximum Doppler shift (0.006 nm) of the absorption line would not be sufficient to remove it from the wide solar Lyman-alpha line. The predicted value at the subsolar point of 340 atoms/cm^3 for the previously mentioned sputtering model (ref. 23-17) is far above our detection limit shown in table 23-I.

Thus, efficient surface recombination of solar protons to molecular hydrogen appears to be the most probable explanation for the low atomic hydrogen density. It is reasonable to expect an efficient trapping of kilovolt protons on the lunar surface (ref. 23-18), followed by an upward diffusion of hydrogen atoms. This upward diffusion would promote recombination either within or at the surface of the soil grains. The molecular hydrogen would then be released by the surface at thermal energy. A theoretical model of Hodges (ref. 23-19) predicts H_2 concentrations of 3.6×10^3 atoms/cm^3 at the subsolar point and 2.3×10^4 atoms/cm^3 at the antisolar point.

As shown in table 23-I, the fluorescence in the H_2 Lyman bands from expected density would have escaped detection in the UVS experiment. The expected nighttime density, however, may ultimately be detected by the Apollo 17 neutral mass spectrometer surface experiment (ref. 23-20).

In conclusion, the Apollo 17 UVS experiment has revealed that atomic hydrogen is almost totally absent in the lunar atmosphere. To explain this observation, we believe that nearly 100-percent conversion of solar wind protons to molecular hydrogen probably occurs at the lunar surface. The expected H_2 density would have so far escaped detection. We would also expect that H_2 will predominate over H for the case of Mercury if its atmosphere is thin enough to allow direct solar wind impact on the surface. A related problem on which this result may bear is the formation of interstellar H_2 on dust particles (refs. 23-21 and 23-22).

LUNAR ALBEDO MEASUREMENTS

During the orbital mission, approximately 50 hr of data were obtained with the UVS observing the sunlit side of the Moon and approximately 50 hr of data were obtained on the dark side. Also during the mission, a rocket experiment conducted by the University of Colorado from the White Sands Missile Range measured the absolute spectral brightness of the Sun in the ultraviolet while the UVS was measuring the sunlit spectrum of the Moon. Thus, we were able to make an absolute measurement of the spectral albedo of the lunar surface.

Before the mission, laboratory measurements had been made of the spectral albedo of lunar dust samples obtained on the Apollo 11, 12, and 14 missions. The laboratory measurements showed that all three lunar samples had an ultraviolet albedo of approximately 2.2 ± 0.2 percent at all wavelengths in the range of 121.6 to 165.7 nm (ref. 23-23). Because almost all minerals are opaque in the spectral region to which the UVS is sensitive, body color plays a small role in the spectral properties of minerals, and refractive index effects probably dominate. Alternatively, metallic sputtering produced by solar wind impact (ref. 23-24) may coat the surface and create the observed grayness in the lunar samples. However, the laboratory-measured albedo is not inconsistent with the assumption that the refractive index, and therefore the mineralogical character of the lunar material, is the factor that controls the far ultraviolet albedo.

Figure 23-6 shows a spectrum obtained from the lunar surface near the subsolar point. The very substantial signals shown, combined with the rocket measurements described previously, permit an accurate measurement of the lunar albedo in the spectral range 118 to 168 nm. This in situ albedo measurement agrees very well with the 2.2-percent value observed in the laboratory.

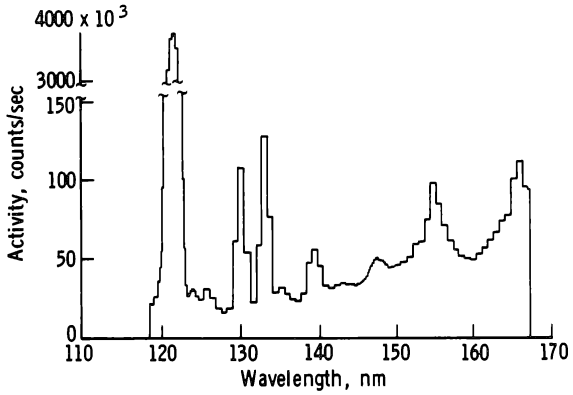

FIGURE 23-6.–Spectrum obtained from UVS observation of the lunar surface near the subsolar point.

Figure 23-7 shows the signal at 147 nm and its variation with lunar longitude during one albedo pass (revolution 28). This curve agrees closely with the behavior of the lunar albedo in the visible region as analyzed by Hapke (ref. 23-25). Figure 23-8 is a plot of the data shown in figure 23-7 divided by the Hapke function for the visible region. Large variations near the terminator are caused by shadowing effects. If the visible Hapke function were the same as the far ultraviolet function, the curve in figure 23-8 would be independent of lunar longitude. In figure 23-9, the residual longitude effect shown in figure 23-8 has been removed by an arbitrary modification of the part of the visible Hapke function that might reasonably be expected to change in the far ultraviolet. Also plotted on figure 23-9 are the normalized data from the next passage across the illuminated surface (revolution 29).

Figure 23-9 demonstrates that the small variations in albedo with longitude are reproducible from one orbit to the next. The most spectacular demonstration is in the crater Neper, which shows an albedo peak in the center of the crater and minimums at the crater edges. However, many other variations are clearly identifiable and are shown to be reproducible in figure 23-9. As might be expected, the variations from point to point on the maria are less pronounced than in other areas. This effect can most clearly be seen in figure 23-7.

Analysis of other bright-side passes demonstrates that the maria show little albedo variation, but there are exceptions (e.g., the southern portion of Mare Crisium). Perhaps the most important observations at this stage of data reduction are that Neper Crater is an exception, that most craters are not distinguishable in the ultraviolet, and that most of the variations in the ultraviolet albedo seem to occur in regions that show little visible variations. Because we believe the albedo observations may have important geological or mineralogical significance, we are continuing data reduction and analysis and plan a program of intercomparison with other lunar observations.

During the passage of the unilluminated portion of the Moon, we observed a reflected Lyman-alpha signal from solar system hydrogen. We have also observed albedo variations in this signal that may be of particular importance because the signal includes

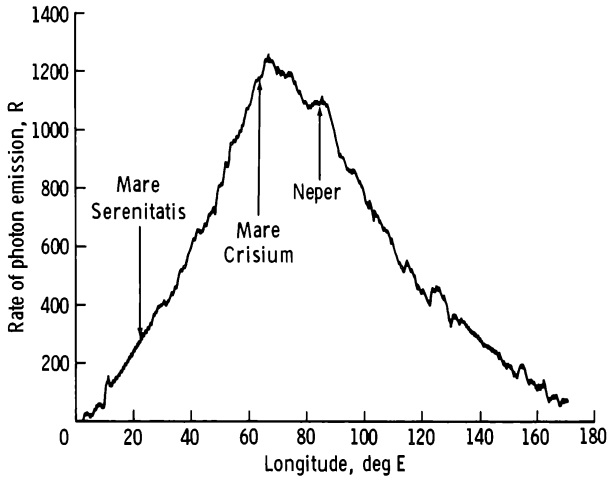

FIGURE 23-7.–Variation of brightness with lunar longitude for the signal observed at 147 nm (fig. 23-6) as the spacecraft traversed the illuminated lunar surface on revolution 28.

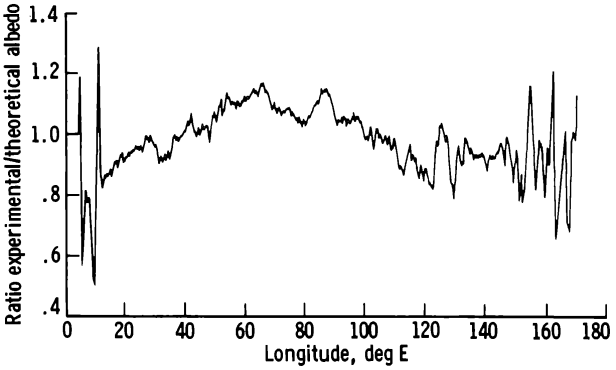

FIGURE 23-8.–Transit data of figure 23-7 divided by visible Hapke function.

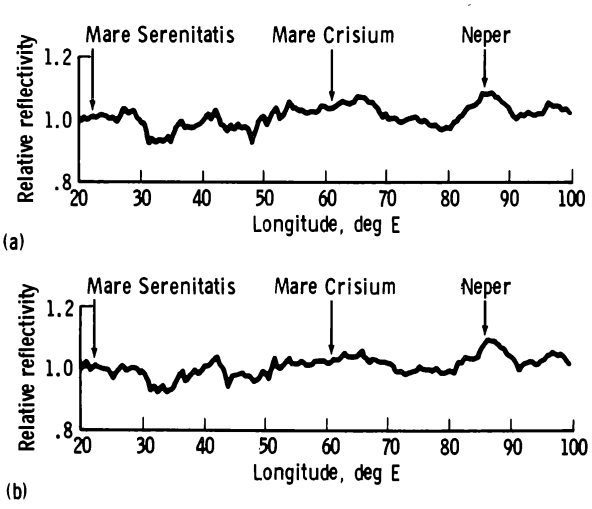

FIGURE 23-9.–Lunar transit data divided by far ultraviolet Hapke function. (a) Revolution 28. (b) Revolution 29.

areas that have not been studied in great detail. However, because the signal is so much weaker than the bright-side signal, little analysis of this data has been performed to date.

OTHER OBSERVATIONS

Twice during lunar orbit, when the spacecraft had just entered the shadow behind the terminator, the spacecraft was oriented so that ultraviolet zodiacal light emissions from the inner solar atmosphere could be observed. These data have only been preliminarily analyzed but generally support the ultraviolet zodiacal light observations by Orbiting Astronomical Observatory 2 (OAO-2) (ref. 23-26).

Several times during TEC, the UVS observed the Earth. Preliminary analysis (ref. 23-27) indicates that the data support the Orbiting Geophysical Observatory IV (OGO IV) orbital observations of the ultraviolet Earth airglow and provide an overall view of the Earth for comparison with other planets.

During TEC, the UVS was operated almost continuously to provide a detailed ultraviolet survey of our galaxy and to observe selected stellar spectra. A massive amount of data was obtained, but its analysis awaits viewing direction information in galactic coordinates. Preliminary analysis of the spectra of isolated bright stars demonstrates that significant data were obtained. The observed ultraviolet spectral distributions agree with previous observations and provide the most precise measurement of absolute ultraviolet brightness obtained to date (ref. 23-28).

The full sky survey described previously also provided a measure of the distribution of solar system Lyman-alpha (121.6 nm) emission that is produced by resonance re-radiation of solar radiation by atomic hydrogen in the solar system. The survey also provided an opportunity to search for a geomagnetic tail of atomic hydrogen downwind from the Sun. These data have not been analyzed.

Once during TEC, the UVS was operating during a molecular hydrogen purge of the fuel cells that produced the ultraviolet spectrum shown in figure 23-10. This spectrum arises from absorption by molecular hydrogen of Lyman-beta and Lyman-gamma solar radiation and fluorescent re-radiation of this energy at longer wavelengths. From knowledge of the brightness of these solar emission features and of the Franck-Condon factors for molecular hydrogen, we have calculated the expected fluorescence spectrum of molecular hydrogen. This theoretical spectrum is shown in figure 23-11 where the intensity of one of the bands has been normalized to the experimental data of figure 23-10. The observed and calculated distributions agree very well. We have also calculated that the observed spectral brightness gives a column density of approximately 1×10^{14} molecules/cm^2, in close agreement with the calculated column density based on a nominal H_2 purge rate and the spacecraft geometry.

The H_2 spectrum provides an internal calibration

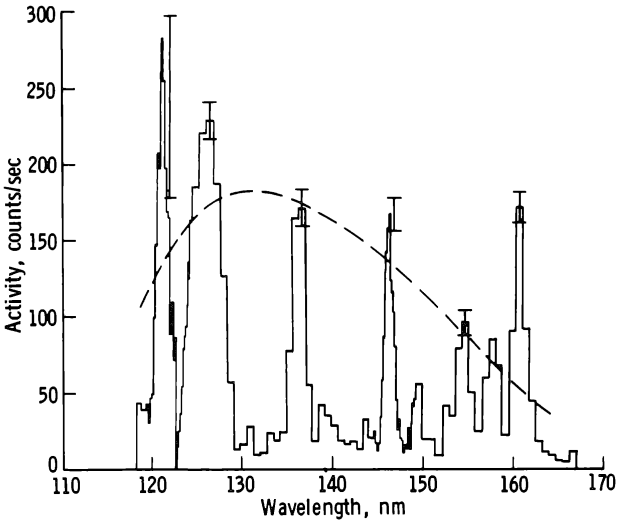

FIGURE 23-10.–Spectrum obtained in TEC during molecular hydrogen purge of fuel cells. The dashed curve represents a brightness of 2 R. The error bars represent 1 standard deviation in the observed counting rate.

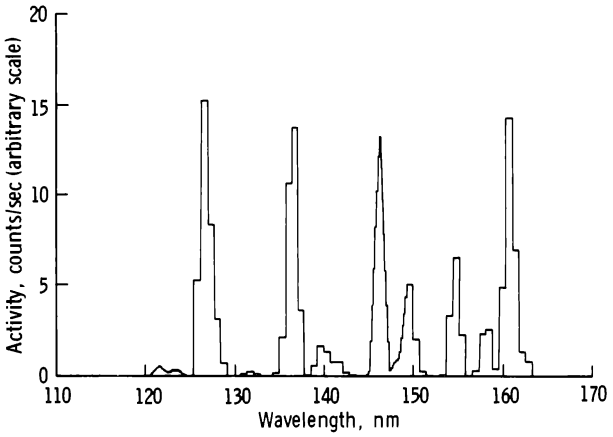

FIGURE 23-11.–Calculated fluorescence spectrum of molecular hydrogen excited by far ultraviolet solar radiation. (Intensity of one band normalized to experimental data (fig. 23-10).)

of the UVS as a molecular hydrogen sensor and gives high reliability to the upper limit on H_2 at the subsolar point discussed in the section entitled "Lunar Atmosphere Observations" and shown in table 23-I. The H_2 observation is also important as an unambiguous means of identifying molecular hydrogen in the atmospheres of planets and comets (ref. 23-29).

REFERENCES

23-1. Fastie, William G.: The Apollo 17 Far Ultraviolet Spectrometer Experiment. The Moon, vol. 7, nos. 1/2, Mar./Apr. 1973, pp. 49-62.

23-2. Johnson, F. S.: Lunar Atmosphere. Rev. Geophys. Space Phys., vol. 9. no. 3, Aug. 1971, pp. 813-823.

23-3. Johnson, Francis S.; Carroll, James M.; and Evans, Dallas E.: Lunar Atmosphere Measurements. Proceedings of the Third Lunar Science Conference, vol. 3, MIT Press (Cambridge, Mass.), 1972, pp. 2231-2242.

23-4. Hodges, R. R.; Hoffman, J. H.; and Evans, D. E.: Lunar Orbital Mass Spectrometer Experiment. Sec. 21 of the Apollo 16 Preliminary Science Report. NASA SP-315, 1972.

23-5. Hoffman, J. H.; Hodges, R. R., Jr.; and Evans, D. E.: Lunar Atmospheric Composition Results From Apollo 17. Lunar Science IV (Abs. of papers presented at the Fourth Lunar Science Conference (Houston, Tex.), Mar. 5-8, 1973), pp. 376-377.

23-6. Hodges, R. R.; Hoffman, J. H.; Yeh, T. T. J.; and Chang, G. K.: Orbital Search for Lunar Volcanism. J. Geophys. Res., vol. 77, no. 22, Aug. 1, 1972, pp. 4079-4085.

23-7. Hodges, R. R.; Hoffman, J. H.; Johnson, F. S.; and Evans, D. E.: Composition and Dynamics of Lunar Atmosphere. Proceedings of the Fourth Lunar Science Conference, Pergamon Press (New York), Dec. 1973.

23-8. Chamberlain, J. W.: Planetary Coronae and Atmospheric Evaporation. Planet. Space Sci., vol. 11, no. 8, Aug. 1963, pp. 901-960.

23-9. Thomas, G. E.; and Krassa, R. F.: OGO 5 Measurements of the Lyman Alpha Sky Background. Astron. Astrophys., vol. 11, no. 2, Apr. 1971, pp. 218-233.

23-10. Barth, Charles A.: Planetary Ultraviolet Spectroscopy. Appl. Optics, vol. 8, no. 7, July 1969, pp. 1295-1304.

23-11. Fairfield, D. H.: Average and Unusual Locations of the Earth's Magnetopause and Bow Shock. J. Geophys. Res., vol. 76, no. 28, Oct 1, 1971, pp. 6700-6716.

23-12. Neugebauer, M.; Snyder, C. W.; Clay, D. R.; and Goldstein, B. E.: Solar Wind Observations on the Lunar Surface with the Apollo-12 ALSEP. Planet. Space Sci., vol. 20, no. 2, Oct. 1972, pp. 1577-1591.

23-13. Leich, D. A.; Tombrello, T. A.; and Burnett, D. S.: The Depth Distribution of Hydrogen in Lunar Materials. Lunar Science IV (Abs. of papers presented at the Fourth Lunar Science Conference (Houston, Tex.), Mar. 5-8, 1973), pp. 463-465.

23-14. Fleischer, Robert L.; and Hart, Howard R., Jr.: Surface History of Lunar Soil and Soil Columns. Lunar Science IV (Abs. of papers presented at the Fourth Lunar Science Conference (Houston, Tex.), Mar. 5-8, 1973), pp. 251-253.

23-15. Geiss, J.; Buehler, F.; Cerutti, H.; Eberhardt, P.; and Filleux, Ch.: Solar Wind Composition Experiment. Sec. 14 of the Apollo 16 Preliminary Science Report. NASA SP-315, 1972.

23-16. Siscoe, G. L.; and Mukherjee, N. R.: Upper Limits on the Lunar Atmosphere Determined from Solar-Wind Measurements. J. Geophys. Res., vol. 77, no. 31, Nov. 1, 1972, pp. 6042-6051.

23-17. Gott, J. Richard, III; and Potter, A. E., Jr.: Lunar Atomic Hydrogen and Its Possible Detection by Scattered Lyman-α Radiation. Icarus, vol. 13, 1970, pp. 202-206.

23-18. Manka R. H.; and Michel, F. C.: Lunar Atmosphere as a Source of Lunar Surface Elements. Proceedings of the Second Lunar Science Conference, vol. 2, MIT Press (Cambridge, Mass.), 1971, pp. 1717-1728.

23-19. Hodges, R. R.: Helium and Hydrogen in the Lunar Atmosphere. J. Geophys. Res., vol. 78, 1973.

23-20. Hoffman, J. A.; Hodges, R. R., Jr.; and Evans, D. E.: Lunar Atmosphere Composition Results from Apollo 17. Proceedings of the Fourth Lunar Science Conference, Pergamon Press (New York), Dec. 1973.

23-21. Spitzer, L.; Drake, J. F.; Jenkins, E. B.; Morton, D. C.; et al.: Spectrophotometric Results from the Copernicus Satellite. IV, Molecular Hydrogen in Interstellar Space. Astrophys. J. Letters, vol. 181, May 1, 1973, pp. L116-L121.

23-22. Hollenbach, D.; and Salpeter, E. E.: Surface Recombination of Hydrogen Molecules. Astrophys. J., vol. 163, no. 1, Jan. 1971, pp. 155-164.

23-23. Lucke, R. L.; Henry, R. C.; and Fastie, W. G.: Far Ultraviolet Reflectivity of Lunar Dust Samples: Apollo 11, 12, and 14. Astron. J., vol. 78, no. 3, Apr. 1973, pp. 263-266.

23-24. Hapke, B. W.; Cohen, A. J.; Cassidy, W. A.; and Wells, E. N.: Solar Radiation Effects on the Optical Properties of Apollo 11 Samples. Proceedings of the Apollo 11 Lunar Science Conference, vol. 3, Pergamon Press (New York), 1970, pp. 2199-2212.

23-25. Hapke, Bruce W.: A Theoretical Photometric Function for the Lunar Surface. J. Geophys. Res., vol. 68, no. 15, Aug. 1, 1963, pp. 4571-4586.

23-26. Lillie, C. F.: OAO-2 Observations of the Zodiacal Light. The Scientific Results From the Orbiting Astronomical Observatory (OAO-2). NASA SP-310, 1972, pp. 95-108.

23-27. Feldman, P. D.; Fastie, W. G.; Henry, R. C.; Moos, H. W.; et al.: Far Ultraviolet Observations of the Earth's Airglow From Apollo 17. Paper presented at 54th Annual Meeting, Am. Geophys. Union (Washington, D.C.), Apr. 1972.

23-28. Henry, R. C.; Moos, H. W.; Fastie, W. G.; and Weinstein, A.: Low-Resolution Ultraviolet Spectroscopy of Several Stars. Paper presented at 16th Plenary Meeting, COSPAR (Konstanz, W. Germany), June 1973.

23-29. Feldman, P. D.; and Fastie, W. G.: Fluorescence of Molecular Hydrogen Excited by Solar Extreme Ultraviolet Radiation. Astrophys. J. Letters, Oct. 15, 1973.